Available online at www.sciencedirect.com

SciVerse ScienceDirect

Ceramics International 39 (2013) 7269–7272

CERAMICS INTERNATIONAL

www.elsevier.com/locate/ceramint

Short communication

$La_{0.8}Sr_{0.2}Cr_{0.5}Fe_{0.5}O_{3-\delta}$ (LSCF)–$Zr_{0.8}Y_{0.2}O_{2-\delta}$ (YSZ) based multilayer membrane for CO_2 decomposition

Wei Fang, Jianfeng Gao*, Chusheng Chen

CAS Key Laboratory of Materials for Energy Conversion, Department of Materials Science and Engineering, University of Science and Technology of China, Hefei, Anhui 230026, China

Received 23 January 2013; received in revised form 7 February 2013; accepted 8 February 2013
Available online 14 February 2013

Abstract

A $La_{0.8}Sr_{0.2}Cr_{0.5}Fe_{0.5}O_{3-\delta}$ (LSCF)–$Zr_{0.8}Y_{0.2}O_{2-\delta}$ (YSZ) based multilayer membrane was fabricated by a combination of dual-layer phase inversion tape casting, slurry coating and co-sintering. LSCF–YSZ was adopted as the oxygen separation layer. A porous YSZ substrate with a continuous transitional finger-like pore structure was prepared, and a LSCF–YSZ active layer with a fine sponge-like pore structure was introduced between the functional LSCF–YSZ oxygen separation layer and YSZ substrate. The asymmetric membrane exhibits good chemical stability and acceptable oxygen permeation under stringent conditions. An oxygen permeation flux of 0.041, 0.068 and 0.15 ml(STP)cm^{-2} min^{-1} was gained at 900 °C for operation under air/argon, CO_2/CH_4 and CO_2/H_2 gradient, respectively. The apparent activation energy for oxygen permeation was 175.61 ± 18.45, 97.21 ± 2.94 and 79.41 ± 6.26 kJ/mol under air/argon, CO_2/CH_4 and CO_2/H_2 gradients respectively. The preliminary results show that the membrane may be promising for applications in the recycling of CO_2 and treatment of hydrocarbons.

Keywords: Oxygen permeable membrane; Asymmetric membrane; CO_2 decomposition

1. Introduction

Oxygen permeable membranes have attracted increasing attention owing to their potential applications in the separation of oxygen from air and conversion of natural gas to syngas [1]. Today, the increase in greenhouse gas emissions, carbon dioxide (CO_2) in particular, is considered to be the main contribution to global warming. Therefore, a combination of carbon dioxide recycling and treatment of hydrocarbons is an attractive option. To explore the feasibility of this idea, a coupling reaction process is proposed in this communication. In an oxygen-permeable ceramic membrane reactor, CO_2 decomposition takes place at one side of the membrane and the oxidation of methane (or hydrogen) occurs at the other side simultaneously or, more clearly, methane (or hydrogen) reacts with oxygen, which permeates through the membrane upon CO_2 decomposition.

There are two main types of oxygen permeable membranes. Single-phase membranes, conducting both oxygen ions and electrons, have been extensively studied for applications in the separation of oxygen from air [2]. Although single-phase membranes exhibit generally high oxygen permeability, their chemical stabilities remain usually problematic, e.g. unstable under a reducing atmosphere for Co-containing ones and very sensitive to CO_2 for Ba-containing ones [3,4]. Dual-phase composite membranes, consisting of an oxygen ionic conductor and an electronic conductor, have attracted increasing interest in recent years [5]. The dual-phase composite membrane shows improved chemical stability, but the oxygen permeability is somewhat lower than that of the single-phase material [6]. Therefore, our group has recently focused on the development of composite membranes, i.e. $La_{0.8}Sr_{0.2}Cr_{0.5}Fe_{0.5}O_3$ (LSCF)–$Zr_{0.84}Y_{0.16}O_{1.92}$ (YSZ), and in this work, the LSCF–YSZ composite was stable under stringent conditions for the 500 h oxygen permeation test [7].

In order to obtain a high oxygen permeation flux, membrane configurations such as asymmetric membranes

*Corresponding author. Tel.: +86 551 63601700.
E-mail address: jfgao@ustc.edu.cn (J. Gao).

0272-8842/$ - see front matter © 2013 Elsevier Ltd and Techna Group S.r.l. All rights reserved.
http://dx.doi.org/10.1016/j.ceramint.2013.02.018

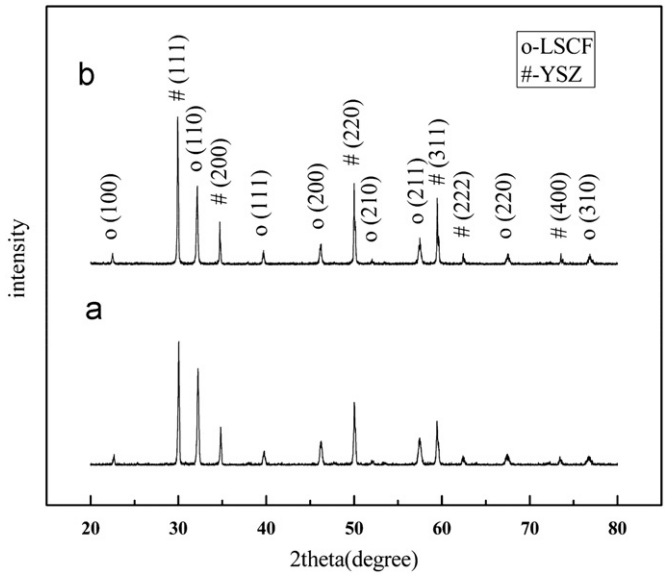

Fig. 1. The XRD patterns of the pre-tested (a) and post-tested (b) functional membrane, (○) LSCF, (#) YSZ.

with reduced membrane thickness are widely studied. For the preparation of asymmetric membranes, the phase-inversion method is a unique technique which has been used frequently in the field of gas separation membranes [8]. In the ceramic systems, usually two macrostructures have been observed, finger-like pores and sponge-like pores [9]. Finger-like pores may provide a route with less resistance for gas transportation, while sponge-like pores may provide a large number of three phase boundaries (TPB) for the electrochemical reactions [10].

In this paper, we report a thin dense $La_{0.8}Sr_{0.2}Cr_{0.5}Fe_{0.5}O_{3-\delta}$.(LSCF)–$Zr_{0.8}Y_{0.2}O_{2-\delta}$ (YSZ) membrane supported on a porous substrate. The porous substrate which was fabricated by the phase-inversion method consisted of a thick finger-like pore structure made of YSZ and a thin sponge-like pore structure made of LSCF–YSZ. Oxygen permeability and chemical stability were investigated.

2. Experimental

A porous support of asymmetric membrane was first prepared by dual-layer phase inversion tape casting. YSZ (d_{50}=0.8 μm, Fanmeiya, Anhui, China) and LSCF powders in a volume ratio of 50:50 were used as the active layer materials. LSCF was synthesized via a conventional solid state reaction route [7]. N-methyl-2-pyrrolidone (NMP, CP, Sinopharm Chemical Reagent Co.), polyethersulfone (PESf, Radel A-100, Solvay Advanced Polymers) and polyvinylpyrrolidone (PVP, K30, Sinopharm Chemical Reagent Co.) were used as the solvent, the binder and the dispersant respectively for the preparation of slurry. The LSCF–YSZ slurry was first applied onto a flat glass plate to form a thin layer using a doctor blade, and then the YSZ slurry was cast on the former to form a thick layer. Subsequently, the glass with the coating was immersed in water. The dried green plate was then cut into discs with a diameter of 20 mm and pre-calcined at 800 °C for 2 h. A functional membrane of LSCF–YSZ was fabricated on the active layer of the support by slurry coating and then co-sintered at 1350 °C for 5 h. The slurry of LSCF and YSZ with the volume ratio of 4:6 was prepared by ball-milling. For comparison, LSCF–YSZ disk-shaped symmetric membrane was prepared by the uniaxial pressing method [11].

The oxygen permeation of the membranes was measured using a home-made setup with an online gas chromatography unit (GC9790II, Fuli, China) equipped with a thermal conductivity detector and two columns, one filled with 60–80 mesh 5 A molecular sieves for oxygen and nitrogen detection and the other filled with 60–80 mesh TDX-01 for H_2, CO and CO_2 detection. In the tests, for the asymmetric membrane, the porous support side was exposed to air (or CO_2) with a flow rate of 30 ml min^{-1} and the functional LSCF–YSZ membrane side was swept with argon (or H_2 or CH_4) with a flow rate of 30 ml min^{-1}. X-ray diffraction (XRD, X'Pert Pro, Phillips, Netherlands) was used to analyze the structure of the pre- and post-tested samples. Morphology of microstructure was characterized by scanning electron microscopy (SEM, JSM-6390LA, JEOL, Japan).

3. Results and discussion

Fig. 1 shows the XRD patterns of the pre- and post-tested membranes. There are only the diffraction peaks of cubic YSZ and perovskite-type LSCF for the functional membrane. It indicates that the used materials are stable during the preparation process and under the operation conditions.

Fig. 2 shows the SEM images of the post-tested membranes. The membrane possesses an asymmetric structure, and the porous support can be divided into two different layers, the thick finger-like pore layer with a thickness of ~1 mm, and the thin sponge-like pore layer with a thickness of ~60 μm (Fig. 2a). The formation mechanism of the finger-like pores can be explained by the viscous fingering phenomenon [12]. When YSZ slurry is in contact with non-solvent (water), an exchange between the solvent (NMP) and non-solvent (water) happens. Local viscosity increases gradually, then the polymer phase (PESf) precipitates, and finally the finger-like pores form in one side of the support. The sponge-like pores are formed in the other side of the support with the solvent of LSCF–YSZ slurry decreases greatly and local viscosity increases, and the viscous fingering ends. The finger-like porous structure could significantly enhance the gas diffusion and offer a high mechanically supporting strength (YSZ mechanical strength: 300 MPa, 25 °C [13]), while the sponge-like structure with fine pores would be in favor of increasing the active sites for the relative surface reactions and improving the surface exchange kinetics. The dense

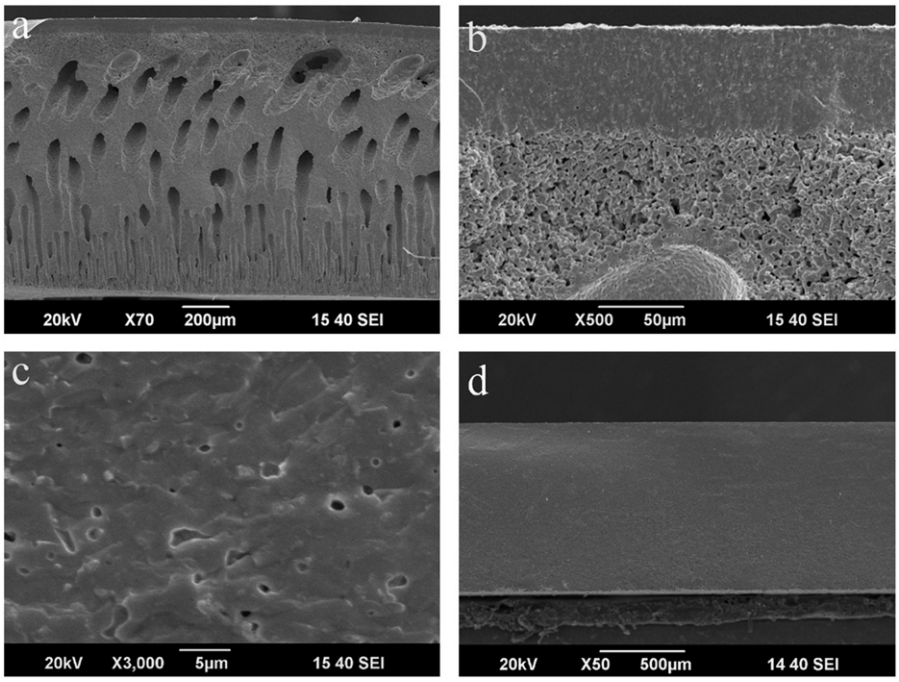

Fig. 2. The SEM images of the post-tested membranes, the cross-sectional view of the asymmetric membrane (a), the interface of the functional membrane and porous support (b), the cross-sectional view of the functional membrane (c) and the cross-sectional view of the symmetric membrane (d).

functional membrane (~60 μm thickness) adheres well on the support (Fig. 2b) and has a gastight bulk (Fig. 2c). For comparison, a membrane (~1 mm thickness) with a symmetric structure is presented (Fig. 2d).

The oxygen permeability of the membranes was examined under air/argon, CO_2/H_2 and CO_2/CH_4 gradients at 750–900 °C. For every tested sample, gastightness was first checked under air/argon gradient at 900 °C. A trace of nitrogen ($\sim 10^{-5}$) was detected in our experiments. Leakage due to imperfect sealing was subtracted when calculating the oxygen permeation fluxes. Oxygen permeation measurements were then carried out under CO_2/H_2 and CO_2/CH_4 gradients. The oxygen permeation flux of a membrane under CO_2/H_2 or CO_2/CH_4 gradient was calculated based on the formation rate of CO at the CO_2 side ($CO_2 = CO + 1/2O_2$).

Fig. 3 shows the temperature dependence of the oxygen permeation rate of the asymmetric membrane. The oxygen permeation rate increases with elevating temperature as expected. At 900 °C, the oxygen permeation rate reached about 0.041, 0.068 and 0.150 ml(STP)cm^{-2} min^{-1} for the membrane under air/argon, CO_2/CH_4 and CO_2/H_2 gradients respectively. According to the Wagner equation [14], a higher oxygen partial pressure gradient results in a larger oxygen flux, and the result is consistent with Liu's work [7]. The calculated activation energy for oxygen permeation was 175.61 ± 18.45, 97.21 ± 2.94 and 79.41 ± 6.26 kJ/mol for the membrane under air/argon, CO_2/CH_4 and CO_2/H_2 gradients respectively. It can be seen that the membrane shows lower apparent activation energy for oxygen permeation under CO_2/CH_4 or CO_2/H_2 than under air/argon gradient. It can be explained by the fact that reducing

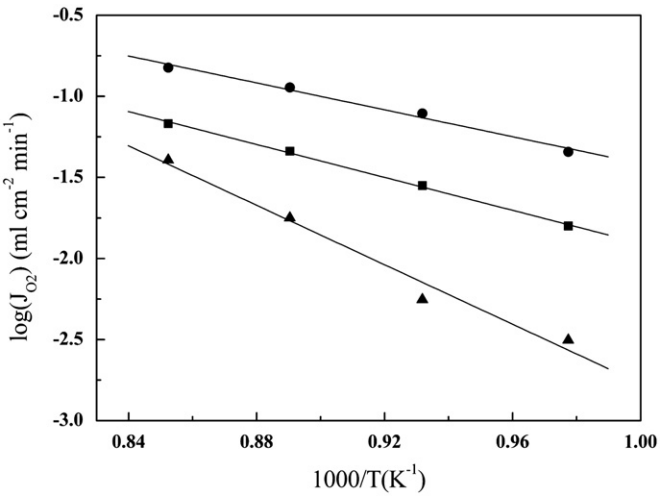

Fig. 3. Temperature dependence of oxygen permeation rate of the asymmetric membrane under (■) CO_2/CH_4, (●) CO_2/H_2 and (▲) air/argon gradients.

atmospheres (e.g. CH_4 or H_2) have enhanced the permeation-limiting role of the relative surface oxygen exchange kinetics [15,17]. Another explanation is that different oxygen partial pressure atmospheres (e.g. CO_2/CH_4 or CO_2/H_2) have led to a change in the oxygen vacancy concentration both on the surface and in the bulk [16,17]. It should be also noted that the oxygen permeation rate is much higher using H_2 as the fuel compared with that using CH_4 as the fuel, while for the case of the apparent activation energy it is the opposite. In our work, no evidence for carbon deposition phenomenon has been

detected on the membrane. Hence, it can be attributed to the relatively low catalytic of LSCF/YSZ for CH_4 reforming. Another reason is possibly due to the fact that H_2 has a higher activity than CH_4 that results in higher reaction kinetics. A similar phenomenon has been also reported in oxide based ceramic anode [18]. In order to improve the performance of LSCF/YSZ membrane for direct methane operation, one of the efficient ways is to introduce transition metals (Ru, Ni, etc.), which show excellent catalytic activity for methane reforming, to the membrane [19]. This work is in progress.

For comparison, LSCF–YSZ disk-shaped symmetric membrane was also measured under CO_2/H_2 gradient. An oxygen permeation flux of 0.026 ml(STP)cm^{-2} min^{-1} was obtained at 900 °C with the symmetric membrane, much lower than that of the asymmetric membrane. For a membrane, when the bulk diffusion is the rate-limiting step, according to Wagner's equation [14], J_{O_2} is reciprocally proportional to the thickness of the membrane. But the data do not follow strictly the value as calculated by the Wagner equation. Therefore, the oxygen permeation of the asymmetric membrane may be not simply controlled by the bulk diffusion, but simultaneously affected by the bulk diffusion and the surface exchange. However, the detail is needed to be studied in the future work.

4. Conclusions

The $La_{0.8}Sr_{0.2}Cr_{0.5}Fe_{0.5}O_{3-\delta}$(LSCF)–$Zr_{0.8}Y_{0.2}O_{2-\delta}$ (YSZ) based multilayer membrane was successfully fabricated by dual-layer phase inversion tape casting, screen printing and co-sintering. It shows acceptable oxygen permeation and excellent chemical stability under CO_2/H_2 and CO_2/CH_4 gradients. The results suggest the membrane has potential applications for carbon dioxide recycling and treatment of hydrocarbons. However, more understanding on the methane catalytic process and the rate-limiting step of the membrane is needed in the near future.

Acknowledgment

This work was supported by the National Natural Science Foundation of China (Grant nos. 21041010 and 21176230).

References

[1] H.H. Wang, C. Tablet, A. Feldhoff, J. Caro, A cobalt-free oxygen-permeable membrane based on the perovskite-type oxide $Ba_{0.5}Sr_{0.5}Zn_{0.2}Fe_{0.8}O_{3-\delta}$, Advanced Materials 17 (2005) 1785–1788.

[2] Z.H. Chen, R. Ran, Z.P. Shao, H. Yu, J.C. Costa, S.M. Liu, Further performance improvement of $Ba_{0.5}Sr_{0.5}Co_{0.8}Fe_{0.2}O_{3-\delta}$ perovskite membranes for air separation, Ceramics International 35 (2009) 2455–2461.

[3] M. Arnold, H.H. Wang, A. Feldhoff, Influence of CO_2 on the oxygen permeation performance and the microstructure of perovskite-type $(Ba_{0.5}Sr_{0.5})(Co_{0.8}Fe_{0.2})O_{3-\delta}$ membranes, Journal of Membrane Science 293 (2007) 44–52.

[4] J.X. Yi, S.M. Feng, Y.B. Zuo, W. Liu, C.S. Chen, Oxygen permeability and stability of $Sr_{0.95}Co_{0.8}Fe_{0.2}O_{3-\delta}$ in a CO_2- and H_2O-containing atmosphere, Chemistry of Materials 17 (2005) 5856–5861.

[5] V.V. Kharton, A.V. Kovalevsky, A.P. Viskup, F.M. Figueiredo, A.A. Yaremchenko, E.N. Naumovich, et al., Oxygen permeability of $Ce_{0.8}Gd_{0.2}O_{2-\delta}$–$La_{0.7}Sr_{0.3}MnO_{3-\delta}$ composite membranes, Journal of the Electrochemistry Society 147 (2000) 2814–2821.

[6] W. Li, J.J. Liu, C.S. Chen, Hollow fiber membrane of yttrium-stabilized zirconia and strontium-doped lanthanum manganite dual-phase composite for oxygen separation, Journal of Membrane Science 340 (2009) 266–271.

[7] J.J. Liu, T. Liu, W.D. Wang, J.F. Gao, C.S. Chen, $Zr_{0.84}Y_{0.16}O_{1.92}$–$La_{0.8}Sr_{0.2}Cr_{0.5}Fe_{0.5}O_{3-\delta}$ dual-phase composite hollow fiber membrane targeting chemical reactor applications, Journal of Membrane Science 389 (2012) 435–440.

[8] Y. Li, T.S. Chung, Y.C. Xiao, Superior gas separation performance of dual-layer hollow fiber membranes with an ultrathin dense-selective layer, Journal of Membrane Science 325 (2008) 23–27.

[9] M.H.D. Othman, Z.T. Wu, N. Droushiotis, G. Kelsall, K. Li, Morphological studies of macrostructure of Ni-CGO anode hollow fibres for intermediate temperature solid oxide fuel cells, Journal of Membrane Science 360 (2010) 410–417.

[10] U. Doraswami, P. Shearing, N. Droushiotis, K. Li, N.P. Brandon, G.H. Kelsall, Modelling the effects of measured anode triple-phase boundary densities on the performance of micro-tubular hollow fiber SOFCs, Solid State Ionics 192 (2011) 494–500.

[11] Y.L. Luo, T. Liu, J.F. Gao, C.S. Chen, $Zr_{0.84}Y_{0.16}O_{1.92}$–$La_{0.8}Sr_{0.2}Cr_{0.5}Fe_{0.5}O_{3-\delta}$ composite membrane for CO_2 decomposition, Materials Letters 86 (2012) 5–8.

[12] B.F.K. Kingsbury, K. Li, A morphological study of ceramic hollow fibre membranes, Journal of Membrane Science 328 (2009) 134–140.

[13] N.Q. Minh, T. Takahashi, Science and Technology of Ceramic Fuel Cells, Elsevier, 1995, pp. 75–80.

[14] S.J. Xu, W.J. Thomson, Oxygen permeation rates through ion-conducting perovskite membranes, Chemical Engineering Science 54 (1999) 3839–3850.

[15] V.V. Kharton, A.L. Shaula, F.M.M. Snijkers, J.F.C. Cooymans, J.J. Luyten, A.A. Yaremchenko, et al., Processing, stability and oxygen permeability of Sr(Fe, Al)O_3-based ceramic membranes, Journal of Membrane Science 252 (2005) 215–225.

[16] H.J.M. Bouwmeester, M.W.D. Otter, B.A. Boukamp, Oxygen transport in $La_{0.6}Sr_{0.4}Co_{1-y}Fe_yO_{3-\delta}$, Journal of Solid State Electrochemistry 8 (2004) 599–605.

[17] H.J.M. Bouwmeester, A.J. Burggraaf, Dense ceramic membranes for oxygen separation, in: A.J. Burggraaf, L. Cot (Eds.), Fundamentals of Inorganic Membrane Science and Technology, Elsevier, Amsterdam, 1996, pp. 435–528.

[18] Q. Liu, D.E. Bugaris, G.L. Xiao, M. Chmara, S.G. Ma, H.C.Z. Loye, et al., $Sr_2Fe_{1.5}Mo_{0.5}O_{6-\delta}$ as a regenerative anode for solid oxide fuel cells, Journal of Power Sources 196 (2011) 9148–9153.

[19] B.C. Enger, R. Lødeng, A. Holmen, A review of catalytic partial oxidation of methane to synthesis gas with emphasis on reaction mechanisms over transition metal catalysts, Applied Catalysis A-General 346 (2008) 1–27.